BJES Basrah Journal for Engineering Sciences

Basrah Journal for Engineering Sciences, Vol. 25, No. 1, (2025), 15-23

Original Article

Journal homepage: www.bjes.edu.iq
ISSN (Online): 23118385, ISSN (Print): 18146120

Performance Evaluation of Single Leg Thermoelectric Module for Different Materials Under Various Operating Conditions

Aqeel M. Uglah [1]*, Khalid B. Saleem [2], Hussein S. Sultan [3], Lioua Kolsi [4]

[1,2,3] *Department of Mechanical Engineering, College of Engineering, University of Basrah, Basrah, Iraq*
[4] *Department of Mechanical Engineering, College of Engineering, University of Hai'l, Hai'l, Saudi Arabia*
E-mail addresses: akeelalzaidy22@gmail.com , khalid.saleem@uobasrah.edu.iq , hussein.sultan@uobasrah.edu.iq, lioua_enim@yahoo.fr

Article Info

Article history:
Received: 14 October 2024
Revised: 26 December 2024
Accepted: 9 January 2025
Published: 16 August 2025

Keywords:
Thermoelectric, Single leg, Peltier cooling, Materials, Potential difference, Power generated.

https://doi.org/10.33971/bjes.25.1.3

Abstract

The thermoelectric behavior of different materials under various conditions has been investigated numerically by using the heat transfer module of the COMSOL Multiphysics software platform. A simulation study of the thermoelectric materials (TEM) performance was created by altering the current applied from 0.1 to 1.0 A and setting the hot side temperature (T_H) as 273 K. The impact of different performance metrics, such as cold side temperature and output voltage, has been proven and investigated. It has been shown that the material of the thermoelectric legs', length of leg, and thickness of electrodes significantly impact the thermal and electrical performance of the thermoelectric (TE) module. Appropriate ranges have been studied in the simulation, such as the amperage values applied to the unit as mentioned above, the length of the leg within a range of 1 to 8 mm, and the thickness of the electrode with different values of 0.1 to 0.5 mm, which will achieve excellent performance for the Thermoelectric unit. Modeling and simulation results demonstrated and revealed the optimal and potential use of bismuth telluride (Bi_2Te_3) as well as lead telluride (PbTe) as suitable for Peltier cooling applications. As for the use of cobalt triantimonide ($CoSb_3$), it is in contrast to the two previous metals, as it is effective and appropriate if applied to power generation. The results are validated with another study from the literature, and there is an excellent agreement with an error rate that does not exceed 0.164%.

1. Introduction

There is a growing need to reduce our dependence on fossil fuels and look for alternative energy technologies that have minimum environmental hazards. Among the results of searches in such alternatives has led to very important research systems wherein thermal energy directly converts to electricity energy and vice versa, attracting researchers worldwide attention. Thermoelectric materials (TEM) can directly and reversibly convert part of the heat energy that passes through them into electrical power and may significantly impact power generation and cooling [1, 2]. What drives us to delve into and research thermoelectric generators (TEGs) are some of the great features that attract many researchers, namely: direct energy conversion, there is no rotating or moving parts, no internal working fluids, and therefore no maintenance, requires no additional costs, and it has a reasonable operating life [3]. Consequently, interest in the TE sector has developed remarkably. However, due to their relatively low efficiency less than 10%, devices in TE have gained low momentum in many markets; improving technologies mean that these efficiencies are on a rise and therefore increasing [4]. One of the areas of recent interest has been the impact nanotechnology technique can have in in changing TE criteria and thereby developing devices' performance [5]. When make coupling for increasing of this efficiency within other features of the TEGs, like, great and higher reliability, simple requirements of maintenance, and the capability for application into the already existing equipment hardware, they turn into a highly desirable prospect. Also, these developments are expected, to drive the market of TE to grow in 2018 from 300$ M to 1.5$ Bn by 2028 almost. As stated, Thus, about 71% of the gas emissions that cause global warming emanate from the generation of power at about 37%, manufacturing industries at 17%, and transport at 17% [6]. Hence, it would mean that a possibility of TE generators applied in such sectors is very feasible. There can be a lot of wasted heat utilized emanating from chimneys, huge furnaces, waste incinerators, and those processes that produced the gases with high temperatures as exhaust to surrounding [7]. TEGs are developed, for instance, gas turbines, exhausts of the automotive, and steel boilers have higher efficiencies with reduced environmental harm due to such processes. Application of TEGs in operations related to power generation, transportation, and industrial systems. are practiced in Wireless sensors, space and wearables. Their important issue always was short life of battery [8]. Recent advances have reduced this power consumption to the order of µW - a level at which TEGs become a realistic technology for considerably extending battery life and even for the complete abolition of batteries. One typical application might be to utilize Wasted heat from heat exchangers plus hot fluid pipes inside buildings to generate suitable power for wireless sensing system that monitor and control the buildings ambient for example, air temperature and value of the humidity [9]. Fundamentally, anywhere there exists a temperature gradient, it is potentially applicable to use a TEG in electrical generation. The most prominent challenges facing the applications of TE power generation are enhancing the efficiency of TEM used in most applications and optimizing the system configuration design

[10]. Martin [11] performed numerical solutions to thermoelectric systems of a single leg of Peltier cooling and thermoelectric generation using Multiphysics code. The boundary conditions implemented were voltage (V = 0) and the temperature (T = 273 K), at the bottom base of the electrode. A geometry of simple cooler consists of single leg p-type semiconductor element, the volume of module of 1 × 1 × 5.8 mm³. Design includes two copper electrodes connected to it from the top and bottom with 0.1 mm in thick for each one. The upper electrode set to 373 K, while the lower electrode set to 273 K. The author outcomes showed that the maximum power output obtained is 1.2 mW. Xiaokai et al. [12] measured TE efficiency of single n-type leg with different lengths and the same composition with temperature set at 100 and 150 °C, respectively in hot-side, while the cold-side temperature used was that of water coolant. The thermoelectric generation by finite-element simulation in COMSOL program was performed by adding two-side temperatures and properties of thermoelectric materials (TEM). The authors results explained that the thermos-electric efficiency of a single leg was 2.57% for 100 ◦C and 3.75% for 150 ◦C hot-side temperatures. Siti Fadzillah et al. [13] experimentally evaluated the performance of a single-leg module. They measured voltage, power, heat flow, and efficiency, all as functions of electric current. Their results showed that all values of the mentioned properties increased when the module operated with bigger temperature differences. Furthermore, they indicated that, in the case of maximum power and efficiency, it reached 0.14 W and 3.1%, respectively, when the module was operated at the hot side with a temperature of 220 °C. Tulaev [14] numerically performed a SiGe superlattice-based single thermoelectric generator is modeled by using the COMSOL Multiphysics software platform. Sample behavior has been simulated when hot and cold surface temperatures change from 338 K up to 388 K. His results indicated that the greatest output power obtained was 0.048 mW. Zheng et al. [15] Studied the high entropy ceramics using this approach and introduced a new concept to develop ultra-performance TE oxides with ultralow thermal conductivity. The experimental results suggested that at 923 K the lowest thermal conductivity can be 1.17 W/m·K, and at 873 K, the figure of merit (ZT) value of 0.2 can be achieved in this sample. Sarabjeet and Yogesh [16] studied the TE effects on a single thermoelectric module consisting of a solo p-type semiconductor numerically by using COMSOL Multiphysics. In their problem settings, they kept the base at a temperature of 300 K plus 0 V of voltage, and at the top surface of the other electrode with 0.7 A of current. Shown in the middle is the resulting temperature distribution. Almost a temperature difference of 70 K is attained, and the highest power output is observed as 1.22 mW. Omar et al. [17] performed a numerical simulation of heat transfer in different materials with solid single-leg modules. They used Software COMSOL Multiphysics to simulate the temperature distribution, electrical potential distribution, power output, and current against temperature across the length of samples. The simulation conducted by them showed that the net temperature difference across lengths for Ca_2FeMoO_6 and $SrTiO_3$ was 191.95 °C and 7.5 °C, respectively, while for Bi_2Te_3, the net temperature difference was -60 °C. Subsequently, they obtained the values of output power for three materials, namely, using an input current of 0.7 A. Thus, the Ca_2FeMoO_6, $SrTiO_3$, and Bi_2Te_3 samples generated an output power of 119 mW, 113 mW, and 34 mW, respectively. Xiaokai et al. [18] studied the effect of TE Legs on the electrical performance of a single leg of TEG using COMSOL Multiphysics in a simulation. Their study was created by altering the hot side temperature from Th = 300 K, 400 K, and 500 K and varying the load resistance from 0 Ω to 20 Ω. Their results showed that the characteristics of the TE leg materials significantly affect how hot or cold the TE module. Moreover, they found that the TEG produces more voltage and power when temperature differences rise. Since then, several research works have tried to optimize the Seebeck coefficient and electric conductivity, while keeping thermal conductivity low, in order to improve the figure of merit for TE materials. However, while dealing with enhancement of TE itself, the main problem in TE is that all three parameters: Seebeck coefficient S, electrical conductivity σ, and thermal conductivity κ, should be considered because these values depend on charge carrier concentration. Another way toward enhancement is optimization of geometry and finding good TE material. Various techniques for improving efficiency and electrical power generation by TEGs have been studied by several researchers. This paper illustrates a simple method for determining the physical properties of a TEC module. The most important thing is to obtain the highest temperature of the cold side of the thermoelectric unit and obtain a suitable electrical potential and thus obtain the highest output power of cooling. Additionally, this article presents the method for selecting the suitable thermoelectrical (TE) module that integrates with a cooling or power generation system. By studying different operating conditions by exposing them to different electrical current ranges or by testing certain engineering designs related to the length and thickness of the thermoelectric unit or with regard to the unit's internal structure by changing the metal from which the thermoelectric leg is formed.

2. Methodology

2.1. Conceptual geometry

The dimensions of geometry model are (1 × 1 × 6) mm³, and it used three various materials as the basic materials for simulation and design, which are Bi_2Te_3, PbTe, and $CoSb_3$. The core of the module consists of the thermoelectric part (Leg). It is covered by two thin electrode plates made of copper with the dimensions (1 × 1 × 0.1) mm³ were used to sandwich the leg, as shown in Fig. 1.

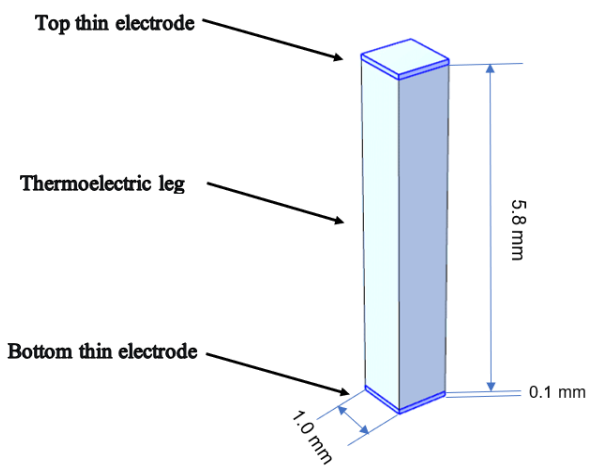

Fig. 1 Core parts of the single thermoelectric module.

2.2. Materials

The three tables below show the main thermoelectric properties for materials that used in the analysis.

Table 1. Properties for Bi_2Te_3 material were utilized as basic input parameters in the current simulation [19].

Properties	Values	Units
Thermal-Conductivity (k)	2.2926	W/(m.K)
Density (ρ)	8150	kg/m^3
Heat capacity (cp)	155	J/(kg.K)
Electrical Conductivity (σ)	0.526×10^5	S/m
Relative Permittivity (ε)	1	-
Seebeck Coefficient (S)	4.51×10^{-4}	V/K

Table 2. Properties for PbTe material were utilized as basic input parameters in the current simulation [20].

Properties	Values	Units
Thermal-Conductivity (k)	1.6	W/(m.K)
Density (ρ)	7740	kg/m^3
Heat capacity (cp)	154.4	J/(kg.K)
Electrical Conductivity (σ)	1.1×10^5	S/m
Relative Permittivity (ε)	1	-
Seebeck Coefficient (S)	2×10^{-4}	V/K
Seebeck coefficient of copper is (6.5×10^{-6} V/K).		

Table 3. properties for CoSb3 material were utilized as basic input parameters in the current simulation [21].

Properties	Values	Units
Thermal Conductivity (k)	5.3	W/(m.K)
Density (ρ)	7310.33	kg/m^3
Heat capacity (cp)	255	J/(kg.K)
Electrical Conductivity (σ)	0.248×10^5	S/m
Relative Permittivity (ε)	1	-
Seebeck Coefficient (S)	1.2×10^{-4}	V/K

3. Mathematical equations of thermoelectric analysis

The TE effect in the steady state can be modeled by the system of equations (1) to (4), where temperature T and voltage U are unknown, while the electric current density J and heat flux q as intermediate variables are three-dimensional vectors, where their units are A/m^2 and W/m^2, respectively. [12, 22, 23]:

$$J = \sigma\,(-\nabla U - S \cdot \nabla T) \tag{1}$$

$$q = -k\,\nabla T \tag{2}$$

$$\nabla J = 0 \tag{3}$$

$$\nabla\,(k\,\nabla T) + \frac{J^2}{\sigma} - TJ \cdot \nabla S = 0 \tag{4}$$

The basic principle technologies of the TE according to Seebeck impact. The value of potential difference resulting between these two junctions based on the type of the materials as well as, the temperature difference between them.

$$S = \frac{\Delta V}{\Delta T} \tag{5}$$

Where ΔV refers to the resulting voltage difference between the two connections and ΔT refers to the temperature difference between the hot surface junction and the cold surface junction (K).

Peltier effect is opposite to the Seebeck effect. The ratio that exists between heat flow rate of two junctions to the amount of direct current that flows in the circuit is called the Peltier coefficient.

$$\pi_{a-b} = \frac{Q}{I} \tag{6}$$

Where $\pi(a - b)$ is Peltier coefficient, Q is cooling or heating rate, I is the current.

The high efficiency of the conversion process of energy obtained at a certain point can be calculate by an important and vital factor, which is the number figure of merit for thermoelectric materials (ZT).

$$ZT = \frac{S^2}{k}\,\sigma T \tag{7}$$

Where S: is the seebeck coefficient (V/K), σ: is the electrical conductivity (S/m) and K: is the thermal conductivity W/m^{2}K.

As well as, the peak efficiency (η) of TEG can be written with referring to the figure of merit.

$$\eta = \frac{T_H - T_C}{T_H}\left[\frac{\sqrt{1+ZT}-1}{\sqrt{1+ZT}+\frac{T_C}{T_H}}\right] \tag{8}$$

Where T_H and T_C represent the temperatures of hot and cold sides respectively.

Thermal conductivity can also be defined as the ability of a body to transmit or spread heat. When two bodies with different temperatures are in contact. As known, the heat is transferred between them and some factors that heat transfer depends on it like temperature gradient, nature of body and thickness etc.

$$k = \frac{Q\,L}{A\,\Delta T} \tag{9}$$

Q: amount of heat transfer that transfer through the body (W).
A: area of the body (m^2).

The boundary conditions used to solve the above governing equations can be set as:

Bottom electrode surface: $T = T_h$
Top electrode surface: Thermal insulation.
Lateral surfaces: Thermal insulation, Electric insulation.
Bottom electrode: $V = Vo$ (Electrically grounded).

4. Grid independency test

The sweep mesh approach creates the module mesh, which enables a finer meshing of the layers of interest, which is the module, the meshing is also specified to have a better resolution and having minimal computation period. The

largest size of element was 0.6 mm, while the smallest size of element was 0.0344 mm. The factor of curvature of 0.6 sets the maximum growth of the element rate to a value of 1.5. Figure 2 below is a pictorial representation of the mesh. Figure 3 is an important step toward the validation of the CFD solution against the present model; it ensures that the convergence criterion for the solution depends on relative residual error and not on further refinement in mesh. Voltage was tested for various mesh element counts starting from 1400 to 6000, and the trend is shown in Fig. 2. The results show that voltage does not change much for a number of mesh elements in the range of 4500-6000. Therefore, a number of mesh elements equal to 4500 will be used in the present work.

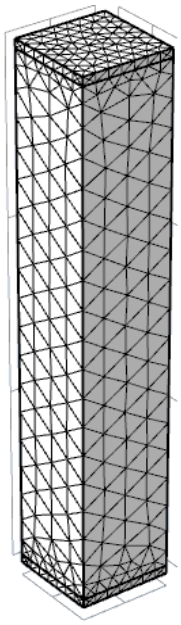

Fig. 2 Mesh design used in the model.

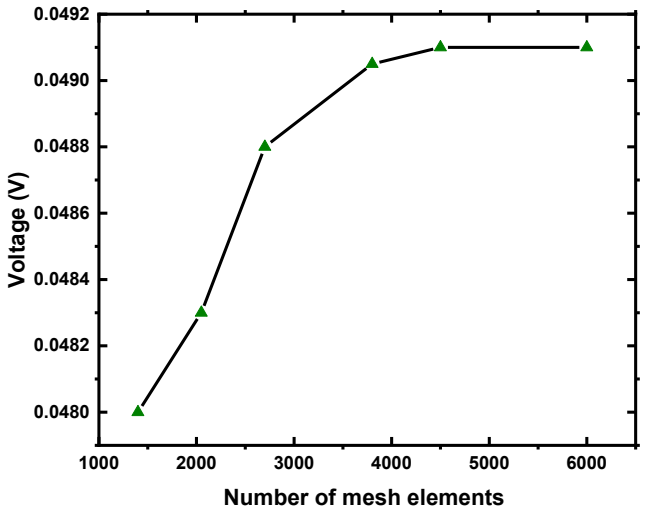

Fig. 3 Grid independence test.

5. Validation of the present work

The present numerical results have been validated with Jaegle [11]. Figure 4 shows an excellent agreement between our simulation results and the correlation equation, and the error rate does not exceed 0.164 %. The parameters that used for validation, both the cold side temperature and electric potential as explained.

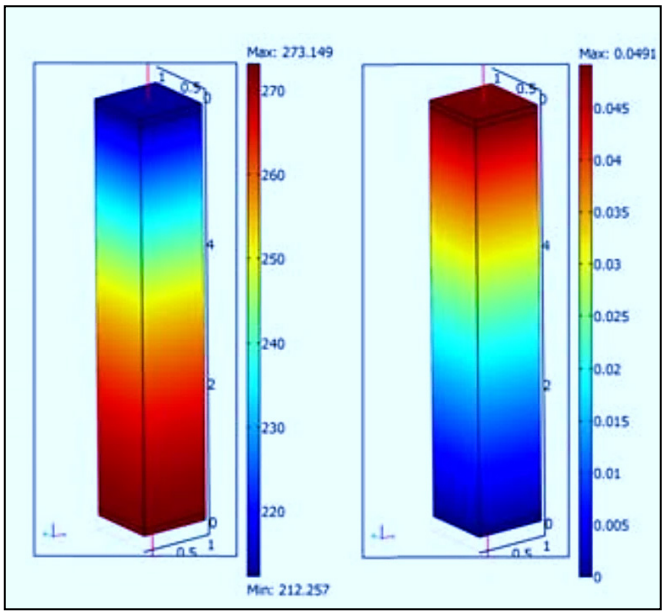

(a) Jaegle [11] results.

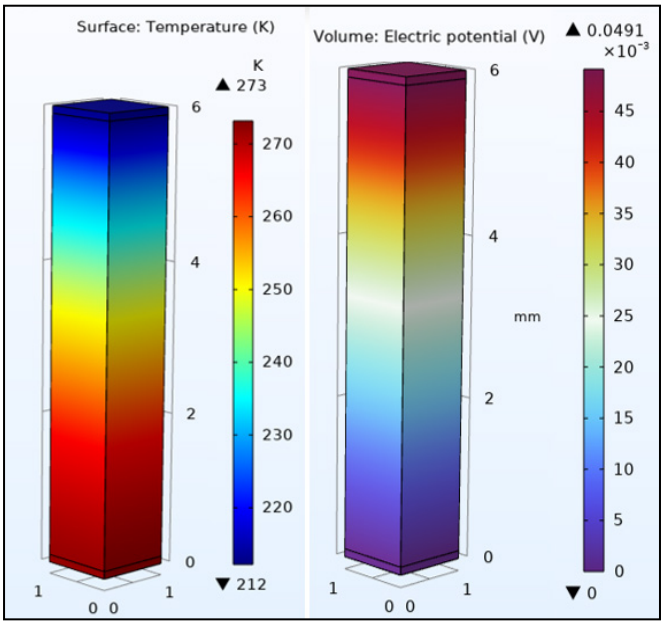

(b) Current study.

Fig. 4 Comparison of current study with Jaegle [11] results.

6. Results and discussion

This section includes the presentation and discussion of numerical results obtained in the current work. The important effects of various materials under different geometrical parameters and operating conditions were discussed, such as the material of the Peltier leg (Bi_2Te_3, PbTe, and $CoSb_3$), the length of the thermoelectrical leg from 1 mm to 8 mm, the thickness of the electrode with ranging of 0.1 mm to 0.5 mm, and multiple values of currents applied from 0.1 to 1.0 A. The findings obtained from the current simulation study were performed by using the heat transfer module of COMSOL program. All simulations were carried out by setting the hot side temperature at the bottom end of the electrode to T_h = 273.15 K.

6.1. Effect of current applied on the cooling temperature

The effect of the current applied on the temperature of the cold side can be established by comparing three materials as follows (Bi_2Te_3, PbTe, and $CoSb_3$) with the same length of leg 7 mm and thickness of the electrode is 0.1 mm, while the applied amperage values change from 0.1 to 1.0 A. Figures 5 (a) and (b) represent the temperature variation of the cold side with the three materials. As observed, the temperature varies for Bi_2Te_3 at 0.1 A from 252.8 K to 211.4 K at 0.7 A, but regarding PbTe from 242.6 K to 189.5 K, while according to $CoSb_3$, from 270.6 K to 327.8 K. When there is an increase in the amperage values applied to the Peltier unit, the amount of electrical energy passing through it will increase, and this increase leads to an increase in the heat that can be transferred from the cold side of the thermoelectric unit to the hot side of it, which leads to more effective cooling. This is seen clearly and visibly. When the amperage values are increased from 0.1 to 0.7 A. It is very important to know the limits of this effect to ensure effective cooling without exceeding the safe limits of the applied amperage values.

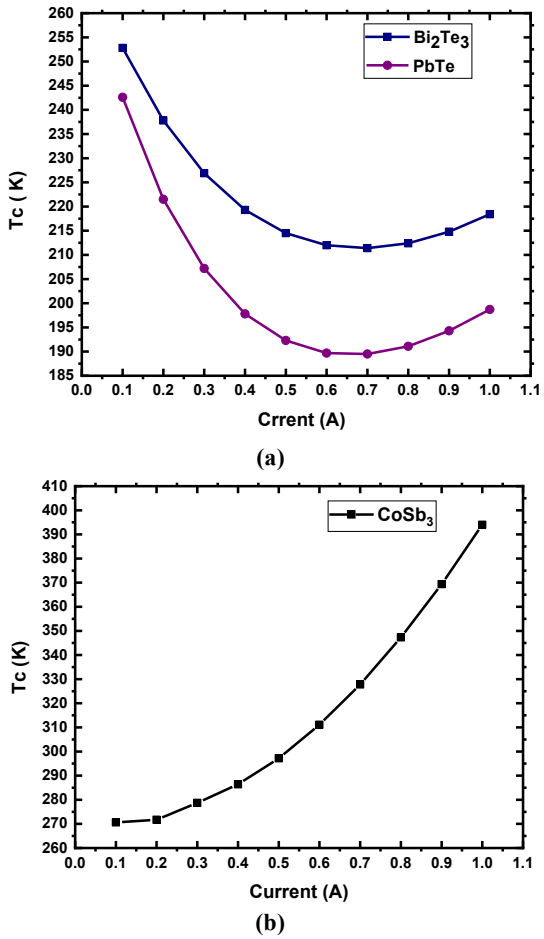

Fig. 5 (a) Cold side Temperature variation of Bi_2Te_3 and PbTe with current applie, **(b)** Cold side Temperature variation of $CoSb_3$ with current applied.

An increase is not always useful, given that applying electrical current values above the specified limit leads to the accumulation of the heat generated and its increase inside the entire unit, which reduces the temperature difference between the hot and cold sides and, thus the cooling effectiveness decreases, and this is noticed when the electric current values exceed 0.7 A, the above analysis concerns Bi_2Te_3 and PbTe as seen in Fig. 5(a). As for $CoSb_3$, the thermal behavior is completely different from the two mentioned materials (Bi_2Te_3, PbTe), and it shows completely different behavior, as with the first two values of the applied current, it shows a modest cooling within simple limits, as is apparent in Fig. 5 (b) below. Then, with the current increase, the temperature increases on the cold side, which was supposed. It obtains effective cooling from it due to its electrical conductivity, which is lower when compared to the previous two materials, which increases the electrical resistance of the metal and thus increases the heat generated. In other words, one cannot expect the Peltier effect to occur in $CoSb_3$. However, this material is well-suited for power generation.

6.2. Effect length of leg on the cooling temperature

The cooling temperature (T_c) is plotted as a function of the length of the leg for (Bi_2Te_3, PbTe, and $CoSb_3$). Different lengths of the thermoelectric leg forming the Peltier unit structure were used, ranging from 1 to 8 mm. What can be observed in Fig. 6 (a) and (b) is that the temperature of the cold side begins to increase with the increase in leg length until it reaches its peak at 7 mm, which shows excellent cooling capacity.

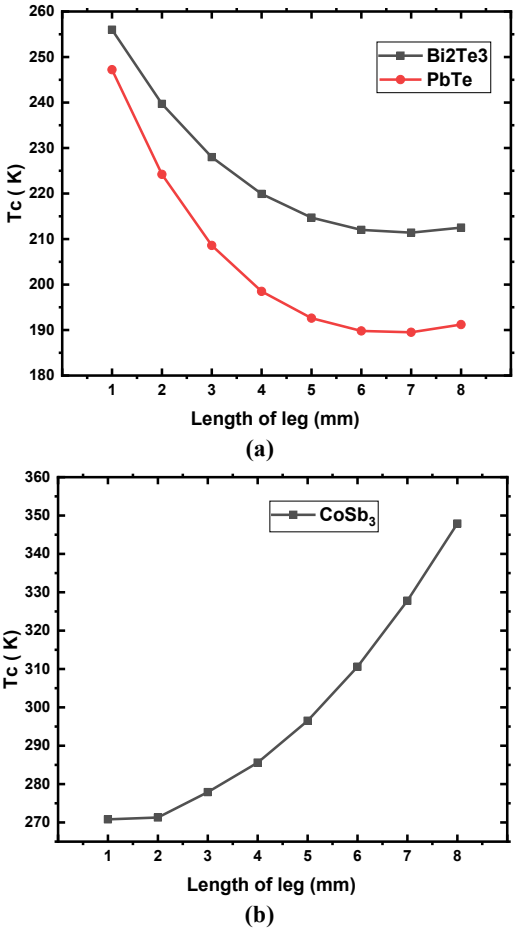

Fig. 6 (a) Cold side temperature variation of Bi_2Te_3 and PbTe with current applied (0.7 A). **(b)** Cold side temperature variation of $CoSb_3$ with current applied (0.7 A).

The ideal length enhances thermal resistance without increasing electrical resistance, which achieves the best cooling performance. The matter is different for $CoSb_3$ because the temperature decreases with increasing length, and this can be attributed to two reasons: the first is the good thermal conductivity it enjoys compared to the previous two metals, and the second is the increase in the electrical resistance of the metal, which leads to wasting energy in the form of heat instead of converting it to cooling.

6.3. Effect of the thickness of the electrode on the cooling temperature

Figures 7(a) and (b) display the relation between the thickness of the electrode and the cooling temperature. Various electrode thicknesses were used, ranging from 0.1 to 0.5 mm. By looking at the graphs below, it can be said that when the electrode of the Peltier unit is thicker, the cooling temperature is lower, which is attributed to the ohmic heat produced by the thicker electrodes as a result of the high electrical resistance that occurs when current passes through them and which doesn't easily transfer from the cold side to the hot side to be dissipated through the metals Bi_2Te_3 and PbTe due to their poor thermal conductivity. Therefore, the electrode thickness of 0.1 mm has the best results compared to other thicknesses. As for the $CoSb_3$ metal, the thicker the copper electrode, the more heat is dissipated from the cold surface due to its good thermal conductivity compared to the previous two metals, allowing for easier and better heat transfer.

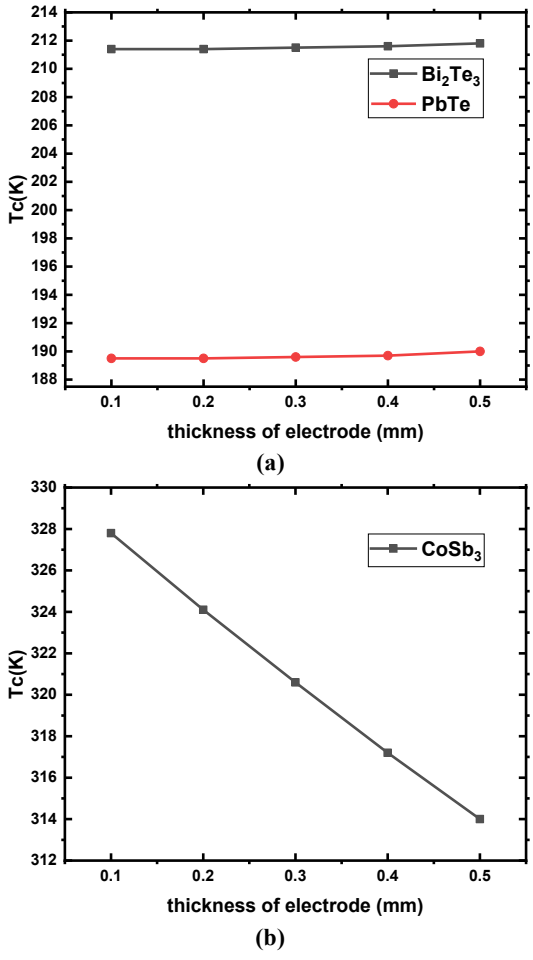

Fig. 7 (a) Cold side temperature variation of Bi_2Te_3 and PbTe with thickness of electrode current applied (0.7 A). **(b)** Cold side temperature variation of $Cosb_3$ with thickness of electrode current applied (0.7 A).

6.4. Distribution of potential

There exists, for any material, a certain potential difference that must be maintained in order to drive a certain amount of electric current across the material. For this present study, an investigation into the simulations for the transfer of heat through the materials serving an applied current, it allowed to investigate the potential gradient that is necessary for causing disorder. and for Bi_2Te_3, it finds that for a cross-sample potential difference of 55.6 mV, one drives current of 0.7 A through the sample. On the other hand, in PbTe, the value of potential difference is 128 mV to derive same current, and with respect to $CoSb_3$, the value is 186 mV. Figures 8, 9, and 10 illustrate these results. This result, in which Bi_2Te_3 requires a much lower potential difference voltage than the other two materials, PbTe and $CoSb_3$, due to their high electrical conductivity, which allows electrons to move easily through the material.

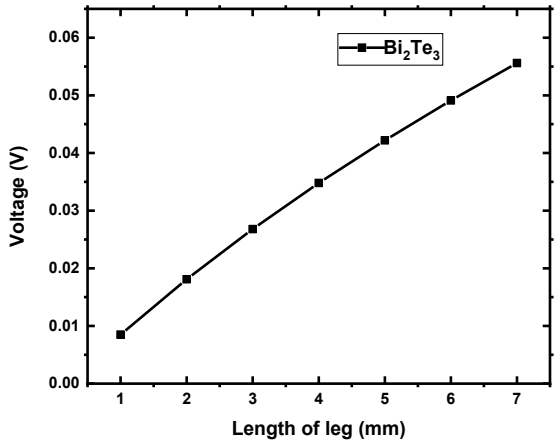

Fig. 8 Voltage profile, V along the 7 mm length of Bi_2Te_3. A voltage difference of 55.6 mV is required to drive a current of 0.7 A through the body of the test sample.

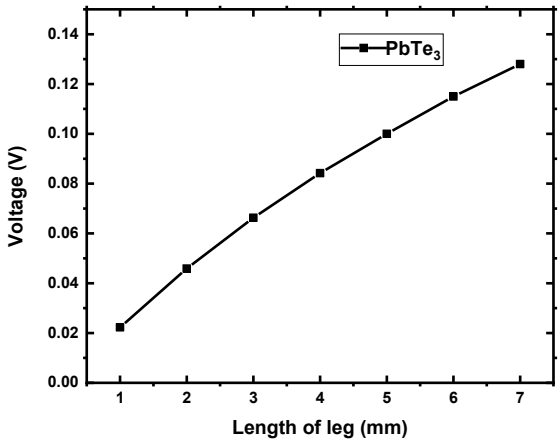

Fig. 9 Voltage profile, V along the 7 mm length of PbTe. A voltage difference of 128 mV is required to drive a current of 0.7 A through the body of the test sample.

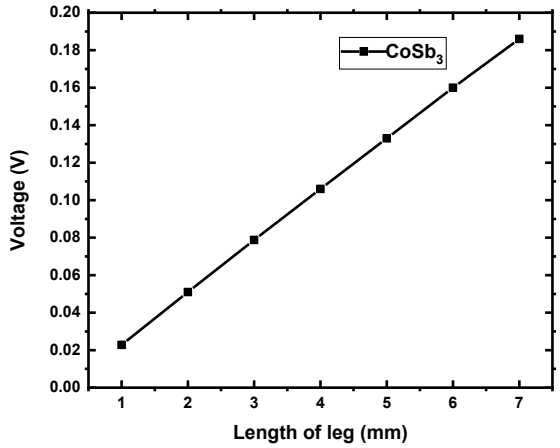

Fig. 10 Voltage profile, V along the 7 mm length of $CoSb_3$. A voltage difference of 186 mV is required to drive a current of 0.7 A through the body of the test sample.

7. Temperature and electric potential contours

Figures 11(a), (b) and (c) below explain the contours of temperature distribution across the length of the samples. This occurs as result of the temperature gradient set up by the direct current flow for the three materials. Figures 12(a), (b) and (c) also show the electrical potential difference due to the flow of current applied to the numerically simulated samples. All three samples with a length of leg 7 mm, 0.1 electrode thickness, Th = 237 K, current applied 0.7 A.

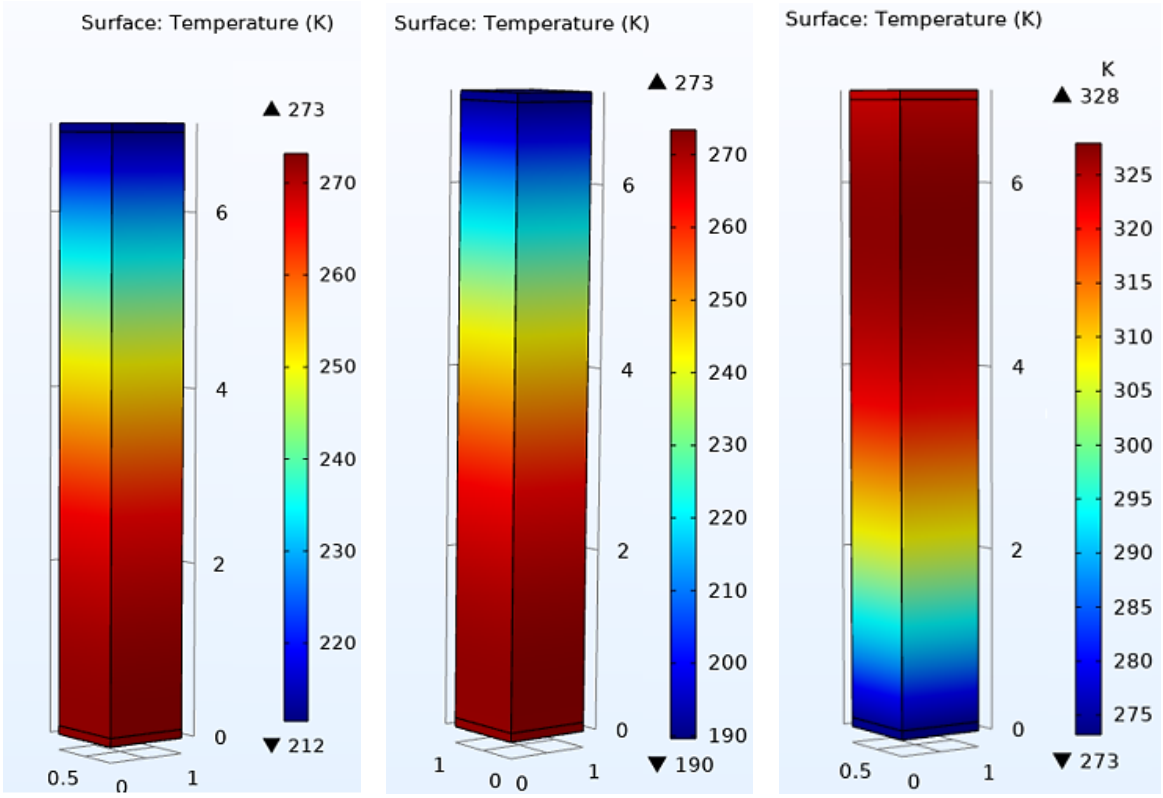

Fig. 11 (a) Temperature variation across the length of Bi_2Te_3. **(b)** Temperature variations across the length of PbTe. **(c)** Temperature variations across the length of $Cosb_3$.

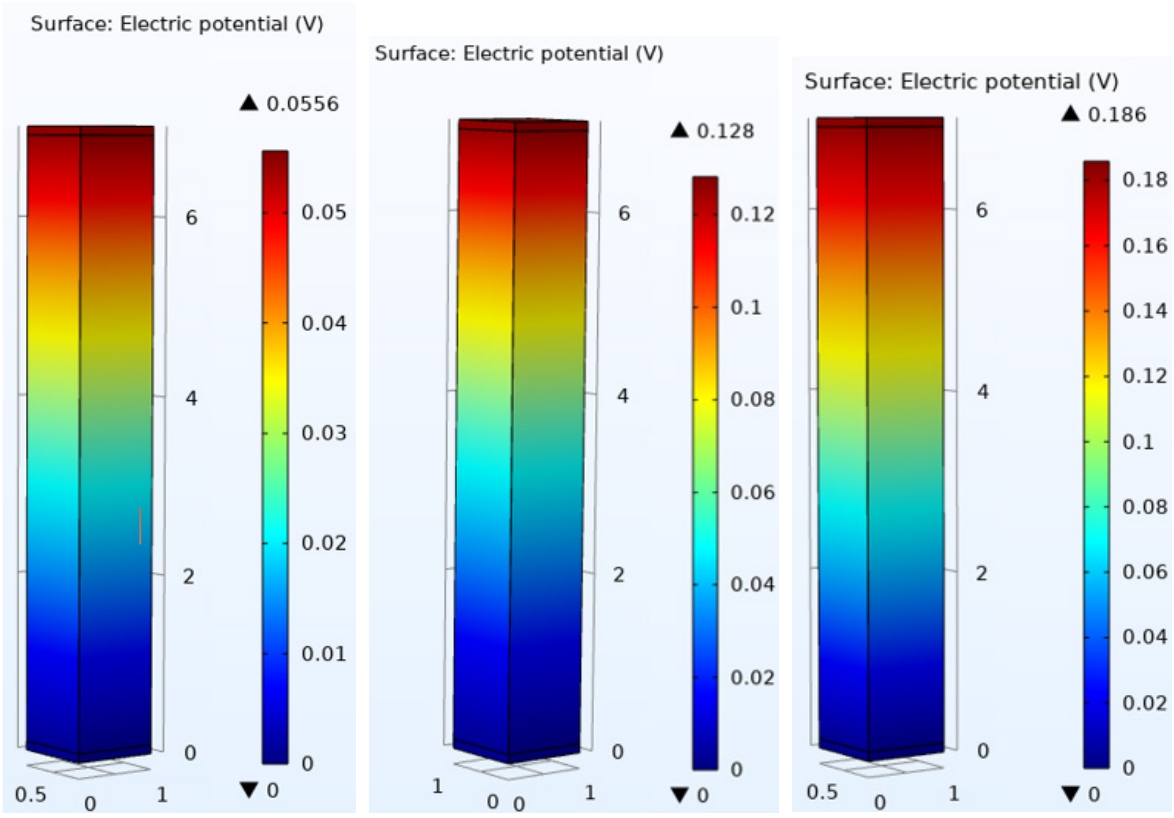

Fig. 12 (a) Electric potential variation across the length of Bi_2Te_3, **(b)** Electric potential variation across the length of PbTe, **(c)** Electric potential variation through the length of $Cosb_3$.

8. Conclusions

In the present work, we have modelling of heat transfer effects and to understand the thermoelectric behavior of certain materials using COMSOL Multiphysics. Besides the determination of optimum current that is essentially required for assumed sample dimensions for effective Peltier cooling, we have understood the potential utilize of Bismuth Telluride nature and Lead Telluride in the applications of Peltier cooling and that of Cobalt Triantimonide material in applications of power generation. Further, as a comparison, we find that Bi_2Te_3 requires a much lesser electric potential to drive the same current through the sample, which would result in better efficiency. However, the fact also remains that the cold side temperature produced is slightly lesser in Bi_2Te_3 as compared to PbTe. It can be inferred Alternatively, in the case of Bismuth Telluride and Lead Telluride, the cold side temperature is observed to be dependent upon the applied current: it is small for low currents and can be enlarged by increasing the applied current. The temperature on the cold side has its maximum at around 0.7 A. It can also be deduced that with application of 3D electrical current, it shows that the temperature in one terminal of the test sample falls much below the room temperature, while the other one remains at lab temperature 273 K, thereby inducing Peltier cooling. Such a conclusion depicts that the two mentioned materials, it can act as good TEMs, as known from past studies. However, it can be interpreted from this simulation that when higher currents beyond 0.7 A are applied, the value of temperature of the cold surface decreases, limiting the Peltier effect. The ideal length of the thermoelectric leg and best electrode thickness were achieved, which give high and effective cooling performance, 7 mm and 0.1 mm, respectively. Finally, this study also shows how the package has been applied to the results of such applications and reflect the predicted behaviors of selected materials as well as assistance in determining optimal parameters and comparative analysis. Obviously, the computer simulations will enable researchers and engineers to further optimize the parameters and enhance process efficiency. They may even investigate new materials and designs to reduce manufacturing or production costs for future studies.

References

[1] X. Hu, A. Yamamoto, M. Ohta, and H. Nishiate, "Measurement and simulation of thermoelectric efficiency for single leg," Vol. 86, Issue 4, pp. 1-8, 2015. https://doi.org/10.1063/1.4916545

[2] T. M. Tritt, "Thermoelectric Phenomena, Materials, and Applications," Annual Review of Materials Research, Vol. 41, pp. 433-448, 2011. https://doi.org/10.1146/annurev-matsci-062910-100453

[3] D. Champier, "Thermoelectric generators: A review of applications," Energy Conversion and Management, Vol. 140, pp. 167-181, 2017. https://doi.org/10.1016/j.enconman.2017.02.070

[4] P. Spriggs and Q. Wang, "Computationally Modelling the Use of Nanotechnology to Enhance the Performance of Thermoelectric Materials," Energies, Vol. 13, Issue 19, 2020. https://doi.org/10.3390/en13195096

[5] C. Xiao, K. Li, J. Zhang, W. H. Tong, Y. Liu, Z. Li, P. Huang, B. C. Pan, H. Su, Y. Xie, "Magnetic ions in wide band gap semiconductor nanocrystals for optimized thermoelectric properties," Materials Horizons, Vol. 1, Issue 1, pp. 81-86, 2014. https://doi.org/10.1039/c3mh00091e

[6] H. Jouhara, A. Żabnieńska-Góra, N. Khordehgah, Q. Doraghi, L. Ahmad, L. Norman, B. Axcell, L. Wrobel, S. Dai, "Thermoelectric generator (TEG) technologies and applications," International Journal of Thermofluids, Vol. 9, 2021. https://doi.org/10.1016/j.ijft.2021.100063

[7] D. Crane, J. LaGrandeur, V. Jovovic, M. Ranalli, M. Adldinger, E. Poliquin, J. Dean, D. Kossakovski, B. Mazar and C. Maranville, "TEG On-Vehicle Performance and Model Validation and What It Means for Further TEG Development," Journal of Electronic Materials, Vol. 42, pp. 1582-1591, 2013. https://doi.org/10.1007/s11664-012-2327-8

[8] Z. Shen, L. Tian, and X. Liu, "Automotive exhaust thermoelectric generators: Current status, challenges and future prospects," Energy Conversion and Management, Vol. 195, pp. 1138-1173, 2019. https://doi.org/10.1016/j.enconman.2019.05.087

[9] R. Freer and A. V. Powell, "Realizing the potential of thermoelectric technology: a Roadmap," Journal of Materials Chemistry C, Vol. 8, Issue 2, pp. 441-463, 2020. https://doi.org/10.1039/C9TC05710B

[10] X. Yang, Z. Dai, Y. Zhao, W. Niu, J. Liua and S. Meng, "Pressure induced excellent thermoelectric behavior in skutterudites $CoSb_3$ and $IrSb_3$," Physical Chemistry Chemical Physics, Vol. 21, Issue 2, pp. 851-858, 2019. https://doi.org/10.1039/C8CP04301A

[11] M. Jaegle, "Multiphysics Simulation of Thermoelectric Systems - Modeling of Peltier-Cooling and Thermoelectric Generation," COMSOL conference 2008 Hannover, No. 6, 2008.

[12] X. Hu, A. Yamamoto, M. Ohta, and H. Nishiate, "Measurement and simulation of thermoelectric efficiency for single leg," Review of Scientific Instruments, Vol. 86, Issue 4, pp. 1-8, 2015. https://doi.org/10.1063/1.4916545

[13] S. F. N. S. Omar, N. Burham, M. Muhamad, and A. A. Aziz, "Effect of Thermoelectric Legs on Electrical Performance of Single Leg Teg using Multiphyiscs Simulation," Vol. 112, Issue 2, pp. 76-85, 2023. https://doi.org/10.37934/arfmts.112.2.7685

[14] A. T. Tulaev, "Simulation of Si / Ge based thermoelectric generator," IOP Conference Series: Journal of Physics, 2019. https://doi.org/10.1088/1742-6596/1326/1/012034

[15] Y. Zheng, M. Zou, W. Zhang, D. Yi, J. Lan, C-W. Nan and Y-H. Lin, "Electrical and thermal transport behaviours of high-entropy perovskite thermoelectric oxides," Vol. 10, Issue 2, pp. 377-384, 2021. https://doi.org/10.1007/s40145-021-0462-5

[16] S. Singh and Y. C. Sharma, "Thermoelectric Effects on $MoSi_2$ with Finite Element Analysis using COMSOL," International Journal of Advanced Engineering Research and Science (IJAERS), Vol. 8, Issue 8, pp. 319-322, 2021. https://doi.org/10.22161/ijaers.88.35

[17] S. F. N. Sidi Omar, N. Burham, and A. A. Aziz, "Simulation of Heat Transfer Response on Single Leg Themoelectric Materials Behaviour," Materials Science Forum, vol. 1055, pp. 69-75, 2022. https://doi.org/10.4028/p-48369p

[18] X. Hu, K. Nagase, P. Jood, M. Ohta, and A. Yamamoto, "Power Generation Evaluated on a Bismuth Telluride Unicouple Module," Journal of Electronic Materials, Vol. 44, pp. 1785-1790, 2015. https://doi.org/10.1007/s11664-014-3556-9

[19] H. J. Goldsmid, "Bismuth Telluride and Its Alloys as Materials for Thermoelectric Generation," Materials, Vol. 7, Issue 4, pp. 2577-2592, 2014. https://doi.org/10.3390/ma7042577

[20] Z. H. Dughaish, "Lead telluride as a thermoelectric material for thermoelectric power generation," Vol. 322, Issue 1-2, pp. 205-223, 2002. https://doi.org/10.1016/S0921-4526(02)01187-0

[21] J. W. Sharp, E. C. Jones, R. K. Williams, P. M. Martin, and B. C. Sales, "Thermoelectric properties of CoSb3 and related alloys," Journal of Applied Physics, Vol. 78, Issue 2, pp. 1013-1018, 1995. https://doi.org/10.1063/1.360402

[22] K. Ahmed, S. Tanvir, R. Al Tahmid, M. I. Sagor, A. Haq, and A. R. Swapno, "Modeling of a Thermoelectric Generator to Produce Electrical Power by Utilizing Waste Heat," 2019 2nd International Conference on Innovation in Engineering and Technology (ICIET), 2019. https://doi.org/10.1109/ICIET48527.2019.9290658

[23] M. Alsheekh, S. E. Najim, and H. S. Sultan, "Experimental, Theoretical and CFD Validations for Solar Powered Atmospheric Water Generation Using Thermoelectric Technics," Basrah Journal for Engineering Sciences, Vol. 21, Issue 2, pp. 17-28, 2021. https://doi.org/10.33971/bjes.21.2.4